Journal Article

# An analysis of the surface quality of AA5182 at different testing temperatures

Schneider, R., Grant, R.J., Heine, B., Börret, R., Burger S. and Zouaoui, Z.

# An analysis of the surface quality of AA5182 at different testing temperatures

R. Schneider[a, b, *], R. J. Grant[a, **], B. Heine[b], R. Börret[c], S. Burger[b] and Z. Zouaoui[a]

[a] *Glyndŵr University, Department of Engineering and Applied Physics, Mold Road, Wrexham, LL11 2AW, UK*

[b] *Aalen University of Applied Sciences, Institute of Surface and Materials Sciences, Beethovenstr. 1, Aalen, 73430, DE*

[c] *Aalen University of Applied Sciences, Centre of Optical Technology, Anton-Huber-Str. 21, Aalen, 73430, DE*

## Abstract

Aluminium sheet metal alloys in the 5000 series exhibit a bad surface quality if deformed at ambient temperatures. The change in surface deviation can be attributed to the Portevin-LeChatelier (PLC) effect, which is not desirable in terms of visual perception. This investigation shows the surface topography of an AA5182 aluminium wrought alloy after specimens were subjected to uniaxial tensile loading at temperatures ranging from 373 to 173 K. The influence of the PLC effect is analysed in terms of surface deviation parameters. The quality of the surface structure is characterised using a Power Spectral Density (PSD) algorithm. It is demonstrated, that the surface quality of an AA5182 aluminium alloy can be significantly enhanced if the material is exposed to sub-zero temperatures.

## Keywords

Aluminium alloy, PortevinLe-Chatelier effect, serrated flow, surface quality, power spectral density

*Corresponding author Tel.: +49 157 36 438 906
*E-Mail address*: robert.schneider.wrexham@hotmail.com or S10002789@mail.glyndwr.ac.uk

** Co-author:
*E-Mail address*: r.j.grant@glyndwr.ac.uk

## 1. Introduction

Due to economic objectives and continuously decreasing fossil-resources the automobile producing industry is forced to minimise the nominal weight of a car body. A weight reduction can be achieved if the car structure is made out of light-weight materials instead of steel [1, 2]. In addition to good corrosion resistance through high passivation affinity, aluminium alloys of the 5000 series show high stiffness to strength values, rigidity and recycling capabilities [3, 4]. Such properties make these alloys eminently suitable for light weight concepts. Nevertheless, aluminium alloys show a limited formability in contrast with, for example, deep drawing steels [5]. Considering the increasing geometric complexity of sheet metal components, manufacturing technologies need to be adapted in order to handle the specific material behaviour [6]. In the case of the strain-hardenable aluminium wrought alloys in the 5000 group, which are exclusively used for inner panels and structural parts, the elongation values are usually appropriate. A negative aspect of AA5000 alloys, containing Mg as the main alloying element, is the formation of stretcher strain markings and parallel bands accompanied by discontinuous plastic deformation [7]. Considering a stress-strain diagram of a strained specimen of the 5000 series (Figure 1), the stretcher strain markings appear at the Lüders-plateau (A) and the parallel bands are seen to exist in the plastic region (B).

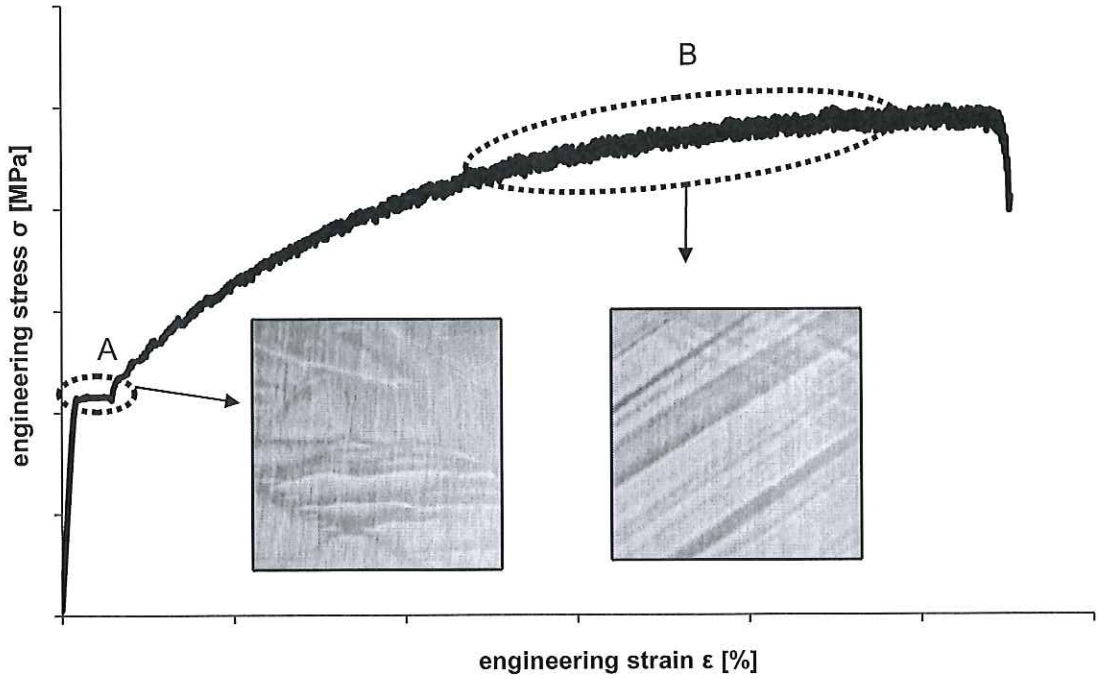


**Figure 1.** Region of stretcher strain markings (A) and parallel bands (B) of a stress-strain curve

The phenomenon of this serrated flow, also known as the Portevin-LeChatelier (PLC) effect, appears at certain temperature ranges and strain rates as evaluated by Pink and Grinberg [8, 9] (Figure 2).

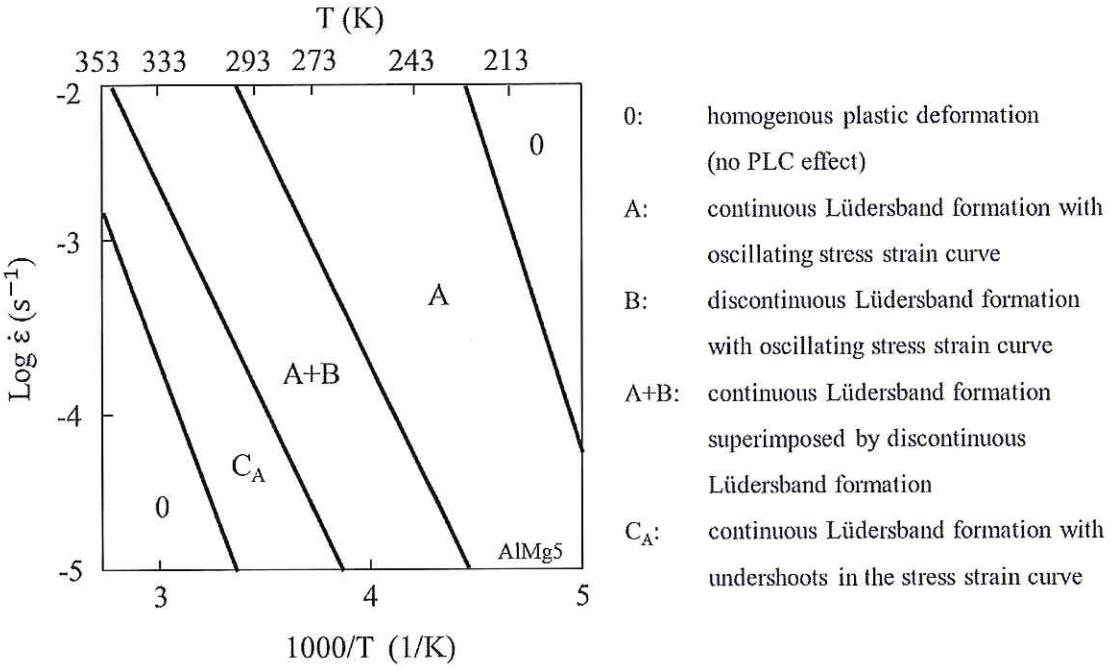


**Figure 2.** Temperature and strain rate dependence of the PLC domain [8]. A, A+B, and $C_A$ indicate different types of serrated flow; 0 illustrates the region with no PLC effect.

Picu [10, 11] described the repeated strain localisation as a mechanism of the negative strain rate sensitivity of the material, which again, is caused by smaller scale phenomena accompanied with interactions between solute and dislocations, referred to as dynamic strain ageing (DSA). This effect is undesirable because the localisations greatly reduce the surface quality. The appearance of the stretcher strain markings (A) and the presence of parallel bands (B) can lead to a surface roughness depth up to 100 µm and 10 µm, respectively [8]. In contrast with stretcher-strain markings, which can be suppressed by certain pre-heat treatments or pre-stretching operations, the alleviation of parallel bands is still a subject of discussion. The surface quality of sheet metal plays an essential aesthetic role if painting processes are considered and it also has bearing on tribological aspects. As a consequence, the sheet metal processing industry resorts to expensive aluminium alloys which do not show this effect when subject to forming operations. So, it is of practical interest to find ways of supressing the PLC effect thus allowing cheaper

aluminium alloys such as alloys in the Al-Mg group to be considered. An option to reduce the macroscopic effect of the DSA may be a low temperature treatment during forming processes. In a previous study [5] it was shown that the mechanical behaviour of commercial aluminium alloys could be significantly enhanced if the testing temperature is decreased. Further, for the aluminium alloy AA5182 it was demonstrated that stress oscillations, accompanied by DSA, disappeared at sub-zero temperatures. In the present research, the interdependence of temperature and the evolution of localisations, i.e. parallel bands, on the surface of commercial aluminium alloy EN AW-5182-H111 is shown. The applicability of the experimental work, using low temperature environments, for industrial applications is discussed.

## 2. Experimental details

### 2.1 Surface analysis

The topographical detection of the specimen surface was accomplished by the confocal measuring system Zeiss Axio CSM 700. Characterisation of the peaks and valleys, accompanied by the parallel bands on the surface was conducted by measuring along three lines ($x_1$, $x_2$ and $x_3$ in Figure 3), which gave the basis for further analysis. The visual demonstration of the specimen topography was obtained by a 2D image ($x_4$ in Figure 3) and is illustrated in a pseudo colour image.

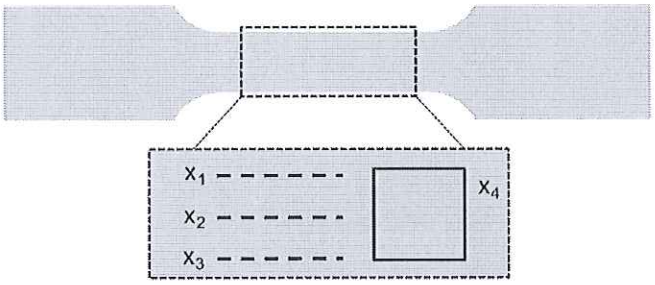


**Figure 3.** Measuring position of the specimen topography

For the quantification of the surface quality the peak-to-valley parameter $P_v$, which expresses the maximum height of a wave profile (Eq. (1)), and the roughness parameter *rms* (Eq. (2)), which describes the micro-topographical surface structure (geometrical error 3rd and 4th order), was used. Figure 4 illustrates the separation of the geometrical errors which occur on a surface.

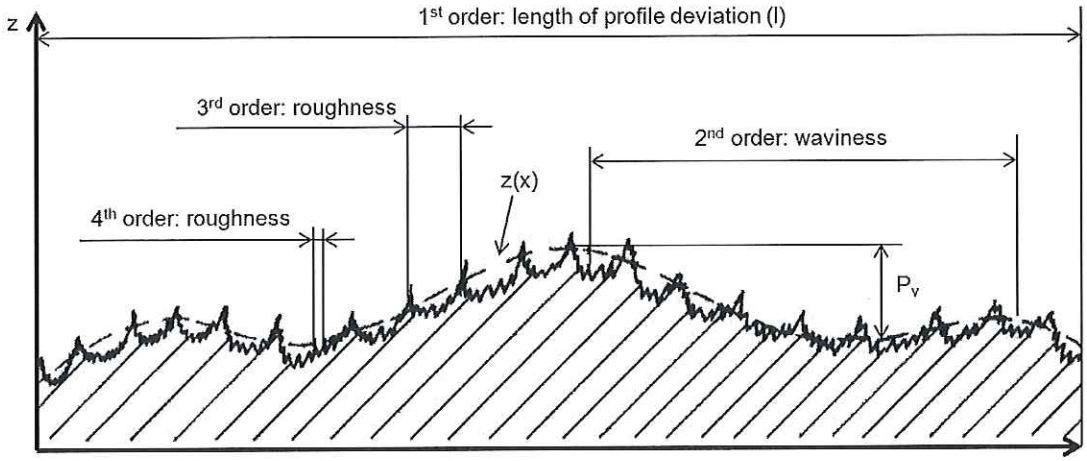


**Figure 4.** Schematic illustration of geometrical errors of a real surface from 1st to 4th order [21]

$$P_v = z_{max} - z_{min} \tag{1}$$

$$rms = \sqrt{\frac{1}{l}\int_0^l |z(x)|dx} \tag{2}$$

For an overview of the surface structure a Power Spectral Density (PSD) algorithm was used where the *normalised surface amplitudes* squared are plotted against *surface wavelength*. Thereby, non-smooth asymmetric distribution functions are compartmentalised into low spatial frequencies (LSFR), mid spatial frequencies (MSFR) and high spatial frequencies (HSFR) [12, 13, 14]. In that way, the transition of the wavelengths provides an easily identifiable assessment of the impact of the forming operation in terms of a measured surface quality.

### 2.2 Testing procedure

A set of experimental tests were conducted based around a tensile testing machine using the wrought aluminium alloy EN AW-5182 in H111 condition [15]. The chemical composition (wt %) of the alloy is Si (0.20 %), Fe (0.35 %), Cu (0.15 %), Mn (0.35 %), Mg (4.40 %), Cr (0.10 %), Zn (0.25 %), Ti (0.10 %) and Al (balance). Flat specimens of 1.00 mm thickness, 12.50 mm width and 50 mm gauge length ($A_{50}$) according DIN 50125 [16] were machined. Tensile testing was carried out within a temperature range from 173 to 373 K at a crosshead velocity of $v = 8.3 \times 10^{-4}\ m/s$ (initial strain rate $\dot{\varepsilon} = 1.67 \times 10^{-2}\ s^{-1}$). The specimens were loaded until fracture to obtain the maximum surface deviation at each testing temperature. Further experimental details

concerning the tensile testing procedure and material parameters can be found in [5]. Since topographical deviations, caused by sheet rolling e.g. mill finish or electrical discharge texture (EDT) (see Figure 5), constitute stress raisers it was perceived that they might influence the PLC bands [17]. The initial EDT surface indicates an *rms* value of 1.63 µm and a $P_V$ value of 7.96 µm. The surfaces of the specimens were thus polished (Figure 6) and as a result, fluctuation-induced serrations and therefore systematic errors were minimised. Through the polishing process the *rms* parameter could be enhanced to 0.16 µm and a $P_V$ of 4.54 µm respectively.

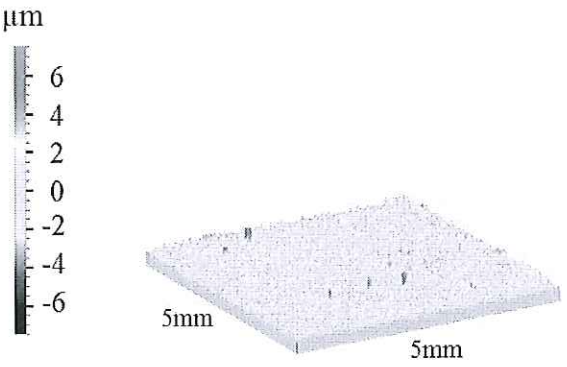


**Figure 5.** Initial EDT surface deviation

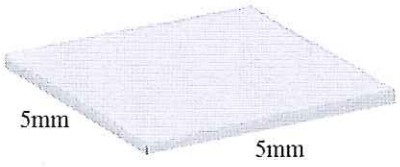


**Figure 6.** Surface deviation after polishing

## 3 Results and Discussion

### 3.1 Temperature impact on surface topography

It should be highlighted that generally the diffusivity of the dissolved atoms is decelerated at low temperatures. Therefore, the interaction between solute and dislocations, resulting in strain localisations, is depressed as temperature is reduced [5, 10]. Figure 7 shows the temperature dependency of the surface deviation parameters $P_V$ and *rms*. For comparison and as a reference of the initial EDT surface quality (delivery condition of the aluminium alloy sheet) a dotted line for $P_V$ and a chained-dotted line for *rms* are employed in the graph. Additionally, for the sake of completeness and to demonstrate the maximal achieved elongation values for the specimens at corresponding testing temperature, the fracture elongation parameter $\varepsilon_f$ is included.

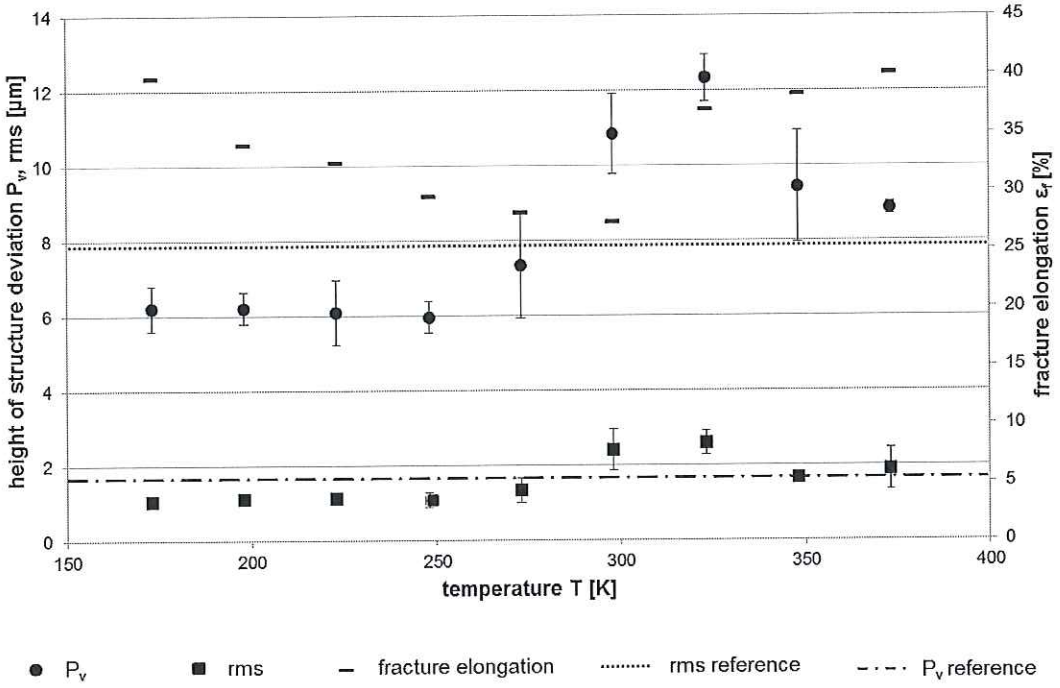


**Figure 7.** Temperature dependence of $P_v$, *rms* and $\varepsilon_f$ values

It can be seen that the roughness values exceed the reference line at temperatures $T \geq 298$ K. The increase of the roughness usually does not detract from the visual appearance of the surface, but indicates the existence of pitting, which may influence tribological processes during sheet metal forming due to rise of the friction coefficient [18]. Below 298 K a certain surface roughness could be obtained which is at least as good as the delivery condition. However, the $P_v$ value, which is in fact a localisation indication parameter, has a greater influence on topography in terms of visual perception. The graph shows that the wave profile height of the surface reaches a maximum at 323 K to a value of around 12.50 µm. A reduction relative to the $P_v$ reference value, which is almost 8µm, can be achieved between testing temperatures of 273 and 248 K. This result fits quite well with the assertion of [19], where a mathematical formulation was developed which expresses the critical temperature $T_{crit}$ of the PLC domain as dependant on the forming velocity (see Eq. (3)).

$$T_{crit}\,[°C] = log_{10}(\dot{\varepsilon}[s^{-1}]) \times 18.8 + 13.8°C \qquad (3)$$

The contrast of the maximum manifestation of the PLC effect and the transition to a smoother surface topography is shown in Figure 8 (*rms* = 2.59 µm; *Pv* = 12.50 µm) and Figure 9 (*rms* = 1.33 µm; *Pv* = 7.34 µm). Considering the surface deviation

parameters $P_v$ and *rms* a relationship with the $\varepsilon_f$ values has not been able to be identified.

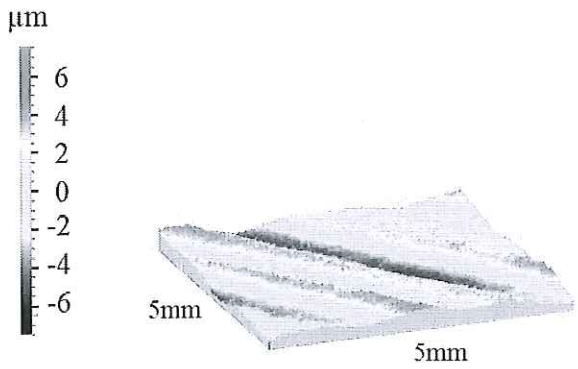


**Figure 8.** Surface deviation at T = 323K

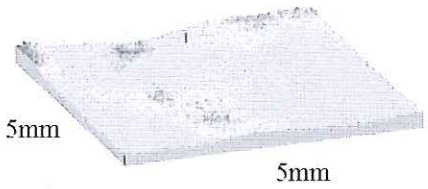


**Figure 9.** Surface deviation at T = 273K

It should be emphasised that a comparison between the intensity of serrations on a stress-strain curve and its corresponding surface quality needs to be treated with caution. *Pink and Grinberg* [8] showed that the intensity of accompanied serrations and therefore the visualisation of the PLC effect on a stress-strain curve, is predominantly dependant on the stiffness of the tensile testing machine. By way of illustration, Figure 10 shows two tensile tests carried out by using two tensile testing machines, differing by way of their stiffness. The tests were conducted at room temperature and the same testing conditions were chosen. It is evident that the stress drops measured by the tensile testing (*TT*) machine 1* ($\Delta\sigma_1 \approx 6$ MPa) is less pronounced than the serrations obtained by the *TT* machine 2** ($\Delta\sigma_2 \approx 60$ MPa), although the surface quality was judged to be identical. The specimen tested with *TT* machine 2 shows a reduced $\varepsilon_f$ value. This is due to the sensitive response of the tactile strain gauge (leading to a dynamic test and therefore to a reduction of the elongation value).

*) Zwick Z100

**) Shimadzu AGC-10/TC

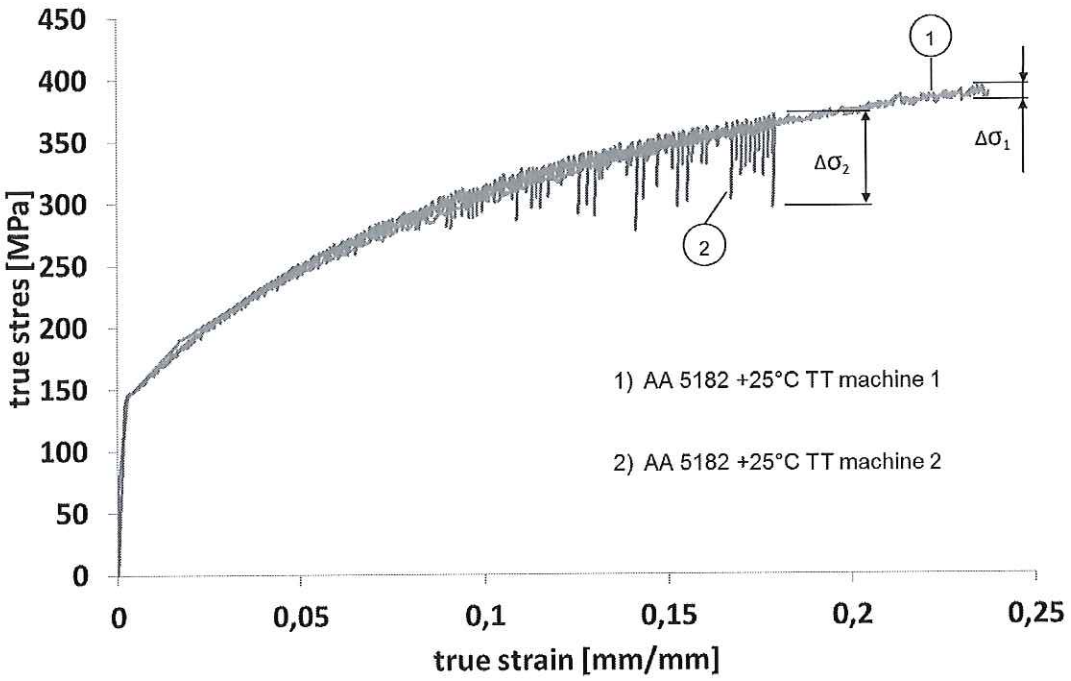


**Figure 10.** Effect of different measuring equipment on serrations in a stress-strain diagram

### 3.2 Power spectral density (PSD) analysis

For characterising the changes of the specimen surfaces, a power spectral density (PSD) analysis is applied (Figure 10). Here, the specimen showing the maximum surface deviation (at $T$ = 323 K) and the specimen where the PLC effect was apparently suppressed (at $T$ = 248 K), were taken into account. Dependent on the surface condition or applied temperature, the spatial frequencies are shifted to higher or lower levels. Therefore, to clarify the impact of the temperature treatment on surface structure, a polished unstrained specimen is taken as a reference as shown in Figure 11 (Characteristic 4). If the surface of an elongated specimen is considered it becomes evident that the PSD characteristic in the *HSFR* and *MSFR* region (outlining the micro-topographical surface structure [12]) is almost identical (see Characteristic 1 to 3 in Figure 11). A pronounced difference in the PSD characteristic can be seen for the surface of the elongated specimen in the *LSFR* region, where visible surface deviations with higher wavelengths λ are indicated [20]. Characteristic 1 (testing temperature T = 323 K) indicates the highest divergence. This result relates to the $P_v$ value introduced in Figure 7. Considering the delivery condition of the

AA5000 material surface (EDT condition) and the surface quality at a deformation temperature of $T$ = 248 K, there is little difference at wavelengths $\lambda \geq 1$ mm.

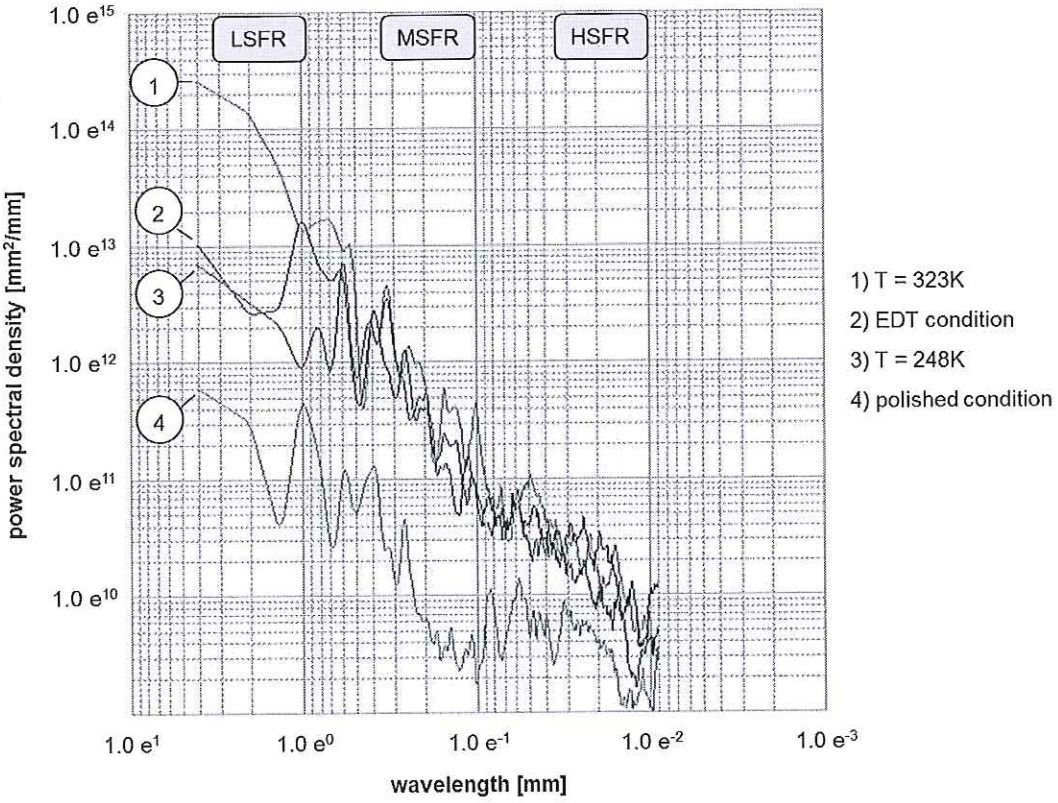


**Figure 11.** Power Spectral Density (PSD) diagram of different surface conditions and testing temperatures

## 4 Conclusions

A Power Spectral Density evaluation was carried out as a new approach for the surface analysis of aluminium sheet metals tested at various temperatures and surface conditions. With this technique the surface topography and its influences on visual perception can be clearly demonstrated. The Portevin-LeChatelier effect and the accompanied strain localisations can be suppressed at forming temperatures $T \leq 273$ K, where a surface quality is achieved which is as good as the delivery condition of the aluminium sheet material. This advantage may be used for the sheet metal processing industry to apply aluminium alloys in the 5000 series for, by way of example, automobile outer skin applications which previously could not be used due to a poor surface quality.

## References


[1] H. Wang, Y.-b. Luo, P. Friedman, M.-H. Chen and L. Gao, "Warm forming behavior of high strength aluminum alloy AA7075," Trans. Non. Met. Soc. 22 (2012) 1-7.

[2] K.-F. Dössel, "OEM-Serienlackierung bei niedrigen Temperaturen," Journal für Oberflächentechnik 53-3 (2013) 20-24.

[3] J. R. Davis, Corrosion of Aluminium and Aluminium Alloys, Ohio: ASM International, 2000.

[4] W. S. Miller, L. Zhuang, J. Bottema, A. J. Wittebrood, P. De Smet, A. Haszler and A. Vieregge, "Recent development in aluminium alloys for the automotive industry," Mat. Sci. Eng. A280 (2000) 37-49.

[5] R. Schneider, B. Heine and R. Grant, Mechanical Behaviour of Commercial Aluminium Aluminium Wrought Alloys at Low Temperatures, Croatia: Intech, 2014.

[6] R. A. Antunes and M. L. de Oliveira, "Materials selection for hot stamping automotive body parts: An application of the Ashby approach based on the strain hardening exponent and stacking fault energy of materials," Mater. Des. 63 (2014) 247-256.

[7] S. Zhang, P. G. McCormick. and Y. Estrin, "The morphology of Portevin-Le Chatelier Bands: Finite Element Simulation For Al-Mg-Si," Acta Mat. 49 (2001) 1087-1094.

[8] E. Pink and A. Grinberg, "Praktische Aspekte des Portevin-LeChatelier-Effektes (1)," Aluminium 60 (1984) 687-691.

[9] E. Pink and A. Grinberg, "Stress Drops in Serrated Flow Curves Of Al5Mg," Acta Met. 30 (1982) 2153-2160.

[10] R. C. Picu, "A mechanism for the negative strain-rate sensitivity of dilute solid solutions," Acta Mat. 52 (2004) 3447-3458.

[11] R. C. Picu, G. Vincze, F. Ozturk, J. J. Gracio, F. Barlat and A. M. Maniatty, "Strain rate sensitivity of the commercial aluminium alloy AA5182-O," Mat. Sci. Eng. A390 (2005) 334-343.

[12] R. Boerret, A. Kelm, H. Thiess and V. Giggel, "ASPHERO5 – Simulation and Analysis of Aspherical Polishing Process," Key Engin. Mat. 364-366 (2008) 488-492.

[13] J. E. Harvey, K. L. Lewotsky and A. Kotha, "Effects of surface scatter on the optical performance of x-ray synchrotron beam-line mirrors," Appl. Opt. 34-16 (1995) 3024-3032.

[14] J. Hol, M. V. Cid Alfaro, M. B. de Rooij and T. Meinders, "Advanced friction modeling for sheet metal forming," Wear 286-287 (2012) 66-78.

[15] DIN EN 515: Aluminium und Aluminiumlegierungen - Halbzeug - Bezeichnung der Werkstoffzustände, Berlin: Beuth Verlag, 1993.

[16] DIN 50125: Prüfung metallischer Werkstoffe - Zugproben, Berlin: Beuth Verlag, 2008.

[17] M. Abbadi, P. Hähner and A. Zeghloul, "On the characteristics of Portevin-Le Chatelier bands in aluminium alloy 5182 under stress-controlled and strain-controlled tensile testing," Mat. Sci. Eng. A337 (2002) 194-201.

[18] F. Ostermann, "Bezeichnung der Werkstoffzustände," in *Anwendungstechnologie Aluminium*, Berlin, Heidelberg, New York, Springer-Verlag, 1998, pp. 352-353.

[19] A. Kamp and S. M. Spangel, "Verfahren zur Herstellung einer geformten Verkleidung aus einer Al-Legierung für Anwednungen in der Luft-und Raumfahrt," Deutsches Patent- und Markenamt. 11 2011 104 398 T5, Filing date: 28.10.2011.

[20] BYK Additives & Instruments, "Einführung ORANGE PEEL / DOI," ALTANA, 2013. [Online]. Available: http://www.byk.com/fileadmin/BYK/downloads/support-downloads/instruments/theory/appearance/de/Einfuehrung_Orange-Peel.pdf. [Accessed 20 06 2013].

[21] H. Braun, H.-D. Dobler, W. Doll, U. Fischer, W. Günter, M. Heinzler, H. Höll, Ignatowitz, T. Röhrer, K. Schilling, W. Röhrer and D. Strecker, Fachkunde Metall 53. Aufl., Haan-Gruiten: Europa Lehrmittel, 1999.